Fuel Cell Catalysis

DOI: 10.1002/anie.201101620

Degradation of Bimetallic Model Electrocatalysts: An In Situ X-Ray Absorption Spectroscopy Study**

Daniel Friebel, Daniel J. Miller, Dennis Nordlund, Hirohito Ogasawara, and Anders Nilsson**

Dedicated to the Fritz Haber Institute on the occasion of its 100th anniversary

Proton exchange membrane fuel cells (PEMFC) could be an important building block for a renewable-energy infrastructure, converting chemically stored energy (e.g., from solar peak production) back into electricity for electric vehicles or stationary off-the-grid applications. An unaccomplished prerequisite for such a development is the availability of cost-efficient electrocatalyst materials, in particular for the oxygen reduction reaction (ORR). Platinum-free catalysts made from earth-abundant materials[1,2] would be desirable, but exhibit too high overpotentials. Nevertheless, the cost of Pt-based catalysts can be reduced by tuning both the morphology and electronic structure to maximize activity. Significant enhancements can be achieved with bimetallic systems where the Pt 5d band is shifted owing to strain and ligand effects.[3–11] However, highly active carbon-supported Pt and Pt-alloy nanoparticles have been successfully tested only on short time scales, whereas degradation occurs under long-term operating conditions through sintering, Pt dissolution, carbon corrosion, and nanoparticle–support detachment.[12,13] Furthermore, the enhanced catalytic activity of bimetallic nanoparticles is often achieved through a specific "core–shell" distribution of constituents,[3,14] which also lacks long-term stability.

Herein we present a study on the anodic oxidation of small Pt islands supported on single-crystal rhodium (111) and gold (111) substrates, using in situ X-ray absorption spectroscopy (XAS) in the high-energy resolution fluorescence detection (HERFD) mode. By depositing ultrathin Pt layers onto a M(111) substrate, we mimic the strain and vertical ligand effects that also occur in Pt alloys, but with better control of structure and element distribution and the highest possible surface sensitivity of the bulk-penetrating hard X-ray probe. Metallic Pt and different Pt oxides can be clearly identified by the shape and intensity of the characteristic maximum ("white line") near the Pt L_3 absorption edge due to $2p \rightarrow 5d$ transitions.[15–17] The spectral resolution in conventional XAS is limited by the Pt 2p core hole lifetime broadening (ca. 5.2 eV), but significantly sharpened spectral features can be obtained with the HERFD technique.[18,19]

The ORR activity for Pt overlayers on various transition-metal substrates has been studied in detail with rotating disk electrode (RDE) measurements,[4] and a volcano plot using the adsorption strength of atomic oxygen as descriptor has been established using density functional theory (DFT).[5,20] While the ORR activities of the two systems studied herein are of the same order of magnitude, they lie on opposite sides of the volcano, exhibiting weaker (Pt/Rh(111)) and stronger (Pt/Au(111)) oxygen adsorption than pure Pt.

However, there is an apparent discrepancy between the theoretically predicted trend[5] and experimentally determined ORR activities for a number of Pt/M(111) systems prepared by redox displacement of underpotential-deposited Cu.[4,21] This disagreement can be explained if, instead of the uniform two-dimensional (2D) monolayers assumed in DFT calculations, redox displacement yields three-dimensional (3D) Pt islands. Indeed, 3D island growth has been confirmed with in situ scanning tunneling microscopy for electrochemically deposited Pt/Au(111).[22,23] On Rh(111), a 2D Pt layer can be grown by ultra-high-vacuum evaporation onto a heated substrate,[24] and we recently studied electrochemical surface oxide formation on such a 2D Pt/Rh(111) sample with in situ HERFD XAS and extended X-ray absorption fine structure (EXAFS) analysis.[25] In contrast, the redox-displacement technique also results in small 3D islands for Pt/Rh(111); this is evident from in situ EXAFS studies (see the Supporting Information). We use this 3D Pt/Rh(111) sample in our comparison with Pt/Au(111) in order to provide a similar Pt morphology.

Interestingly, not only the d-band shifts and corresponding oxygen affinities for Pt/Au(111) and Pt/Rh(111) but also the surface energies of the substrate metals in these systems differ substantially. Au has a significantly lower surface energy than Pt,[26] which explains why Pt cannot be grown on Au in a layer-by-layer mode. Rh, in contrast, has a higher surface energy than Pt. We find that surface and cohesion energies strongly influence the redox chemistry of Pt islands at potentials above 1.0 V (vs. a reversible hydrogen electrode, RHE), where Pt oxides and hydrated Pt cations become thermodynamically stable. Such conditions can occur in various fuel cell operating scenarios[12] and contribute significantly to catalyst degradation.

In situ HERFD XAS measurements on Pt/Rh(111) (Figure 1a) and Pt/Au(111) (Figure 1b) show significant

[*] Dr. D. Friebel, D. J. Miller, Dr. D. Nordlund, Dr. H. Ogasawara, Prof. A. Nilsson
SLAC National Accelerator Laboratory
2575 Sand Hill Rd, Menlo Park, CA 94025 (USA)
E-mail: dfriebel@slac.stanford.edu
nilsson@slac.stanford.edu

[**] This work is supported by the Department of Energy, Office of Basic Energy Sciences, Division of Materials Sciences and Engineering, under contract DE-AC02-76SF00515. This research was partly carried out at the Stanford Synchrotron Radiation Lightsource, a National User Facility operated by Stanford University on behalf of the U.S. Department of Energy, Office of Basic Energy Sciences.

Supporting information for this article is available on the WWW under http://dx.doi.org/10.1002/anie.201101620.

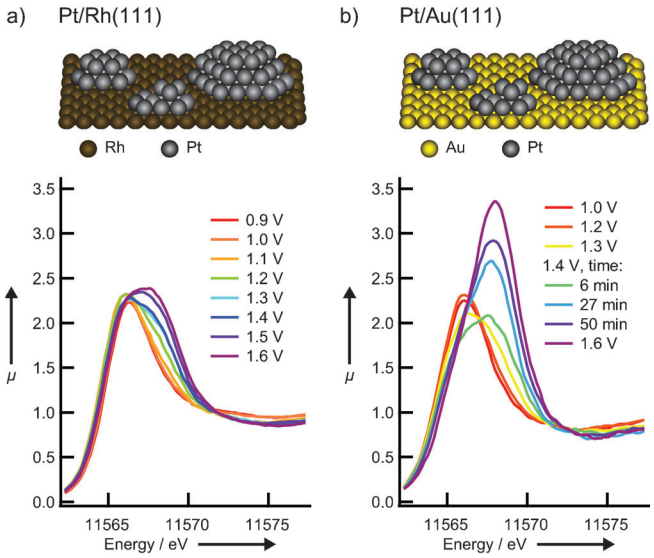

Figure 1. In situ Pt L_3 HERFD XAS for a) Pt/Rh(111) and b) Pt/Au(111) in 0.01 M $HClO_4$. Spectra were recorded in the order of increasing electrochemical potential. For Pt/Au(111) we also show a time series of single XAS sweeps at 1.4 V. μ = normalized absorption.

changes in the white-line region as the potential is increased above 1.0 V. On both samples we initially observe a transition from a narrow absorption maximum at 11566 eV to a much broader peak around 11567 eV; similar changes were observed in our previous study of 2D Pt/Rh(111).[25] However, while this new feature saturates on both 2D Pt/Rh(111) and 3D Pt/Rh(111) upon further increasing the potential, a second transition occurs on Pt/Au(111) after 1.4 V is reached. At this potential, a strong increase of the white-line intensity develops during a time-scale of approximately 40 min, and the absorption maximum shifts to 11568 eV.

By comparison with ab initio multiple-scattering calculations using FEFF8.4[27] for various platinum oxides (Figure 2), it is clear that the high white-line intensities observed for Pt/Au(111) above 1.4 V can only be explained with the formation of Pt^{IV}. The broader appearance and weaker peak intensity in the experimental spectra as compared with the calculations for PtO_2 can be attributed to

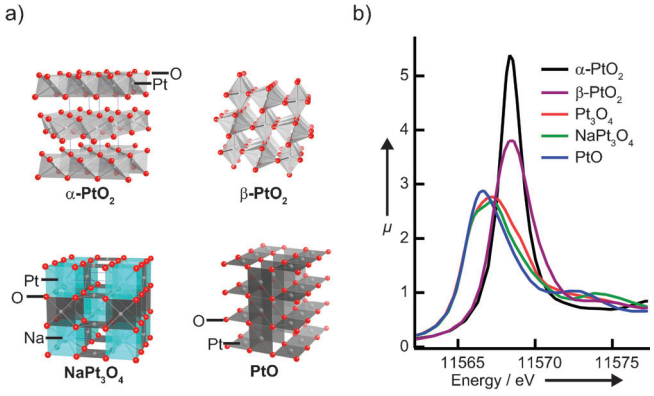

Figure 2. a) Structure models and b) calculated HERFD XAS spectra of different platinum oxides. Calculations were carried out with FEFF8.4.[27]

either additional Pt in lower oxidation states or to a disordered PtO_2 structure.

The potential dependence of the amount of oxide formation can be monitored using integrated white-line intensities as shown in Figure 3a. Oxide formation on Pt/Rh(111) appears sluggish throughout the potential range

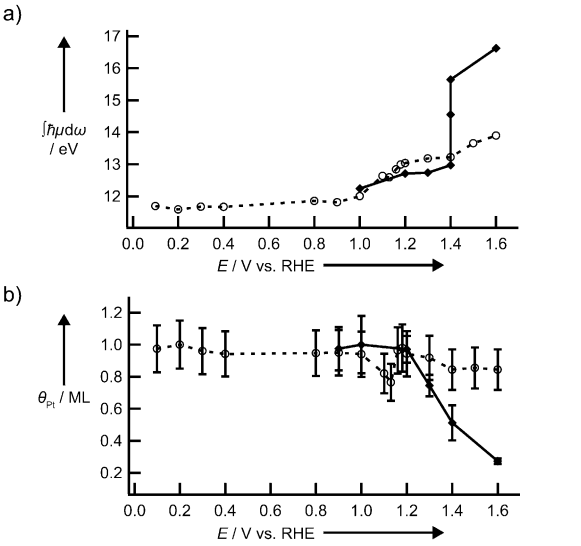

Figure 3. a) Potential dependence of Pt oxide formation for Pt/Rh(111) and Pt/Au(111); the increase of the integrated white-line intensity indicates the extent of Pt oxidation. b) Pt coverage θ_{Pt} determined from relative fluorescence count rates at 11600 eV incident energy, as a function of increasing potentials; note the anodic dissolution of Pt/Au(111). ML = monolayer. Data in (a) and (b) are shown as dashed lines with open circles for Pt/Rh(111) and as solid lines with diamonds for Pt/Au(111).

studied. Similar behavior was found with XAS on 2D Pt/Rh(111)[25] and with in situ X-ray diffraction on Pt(111),[28] and a Pt–O place-exchange mechanism was proposed.[28,29] In contrast, a sharp increase of the average Pt oxidation state can be seen for Pt/Au(111) at 1.4 V, pointing towards a significantly faster phase transition at this potential. Moreover, oxide formation on Pt/Au(111) coincides with Pt dissolution (Figure 3b), whereas dissolution from Pt/Rh(111) is not detectable within uncertainties arising from sample and beam alignment. We conjecture that the rapid oxide growth at 1.4 V is facilitated by an alternative oxidation pathway in which Pt is dissolved as Pt^{2+} with subsequent further oxidation of Pt^{2+} to Pt^{4+}, which precipitates as oxide, thus avoiding sluggish Pt–O solid-state diffusion.

The unusually strong tendency of Pt/Au(111) towards Pt dissolution can be explained with a general destabilization of Pt islands on Au surfaces arising from the surface energy mismatch. Surface Pt tends to be removed in favor of exposing Au, which has much lower surface energy, either at high potentials by anodic dissolution[30] or by diffusion into the Au substrate.[31–33] Pt oxide formation should follow a similar thermodynamic dependence on Pt island stability as dissolution; this relationship, however, may be obscured by the complex kinetics of the Pt–O place exchange. In analogy

to a trend shown for 4d transition metals,[34] increased Pt cohesion in Pt/Au(111) owing to the d-band shift may destabilize subsurface oxygen, a precursor to oxide formation.

In summary, our XAS results clearly show that anodic Pt dissolution is promoted on a Au(111) substrate, whereas anodic polarization of Pt/Rh(111) leads instead to passivation. We can expect Pt/Rh(111) or Pt/Rh nanoparticles to provide good long-term stability under ORR conditions. However, the catalytic activity is suboptimal, and several other substrates with high surface energy, for example, iridium and ruthenium, also shift the Pt 5d band too far toward the weak Pt–O interaction side of the fuel cell volcano plot. Therefore, it may be necessary to find a compromise in ORR catalyst design between high activity and long-term stability.

Received: March 5, 2011
Published online: July 13, 2011

Keywords: ab initio calculations · electrochemistry · fuel cells · heterogeneous catalysis · X-ray spectroscopy

[1] B. B. Blizanac, P. N. Ross, N. M. Markovic, *Electrochim. Acta* **2007**, *52*, 2264 – 2271.
[2] R. Bashyam, P. Zelenay, *Nature* **2006**, *443*, 63 – 66.
[3] P. Strasser, S. Koh, T. Anniyev, J. Greeley, K. More, C. Yu, Z. Liu, S. Kaya, D. Nordlund, H. Ogasawara, M. F. Toney, A. Nilsson, *Nat. Chem.* **2010**, *2*, 454 – 460.
[4] J. L. Zhang, M. B. Vukmirovic, Y. Xu, M. Mavrikakis, R. R. Adzic, *Angew. Chem.* **2005**, *117*, 2170 – 2173; *Angew. Chem. Int. Ed.* **2005**, *44*, 2132 – 2135.
[5] J. Greeley, I. E. L. Stephens, A. S. Bondarenko, T. P. Johansson, H. A. Hansen, T. F. Jaramillo, J. Rossmeisl, I. Chorkendorff, J. K. Nørskov, *Nat. Chem.* **2009**, *1*, 552 – 556.
[6] K. Sasaki, Y. Mo, J. X. Wang, M. Balasubramanian, F. Uribe, J. McBreen, R. R. Adzic, *Electrochim. Acta* **2003**, *48*, 3841 – 3849.
[7] J. Zhang, K. Sasaki, E. Sutter, R. R. Adzic, *Science* **2007**, *315*, 220 – 222.
[8] R. Zeis, A. Mathur, G. Fritz, J. Lee, J. Erlebacher, *J. Power Sources* **2007**, *165*, 65 – 72.
[9] V. R. Stamenkovic, B. Fowler, B. S. Mun, G. F. Wang, P. N. Ross, C. A. Lucas, N. M. Markovic, *Science* **2007**, *315*, 493 – 497.
[10] V. R. Stamenkovic, B. S. Mun, M. Arenz, K. J. J. Mayrhofer, C. A. Lucas, G. F. Wang, P. N. Ross, N. M. Markovic, *Nat. Mater.* **2007**, *6*, 241 – 247.
[11] H. Wolfschmidt, R. Bussar, U. Stimming, *J. Phys. Condens. Matter* **2008**, *20*, 374127.
[12] R. Borup, J. Meyers, B. Pivovar, Y. S. Kim, R. Mukundan, N. Garland, D. Myers, M. Wilson, F. Garzon, D. Wood, et al., *Chem. Rev.* **2007**, *107*, 3904 – 3951.
[13] S. S. Zhang, X. Z. Yuan, J. N. C. Hin, H. J. Wang, K. A. Friedrich, M. Schulze, *J. Power Sources* **2009**, *194*, 588 – 600.
[14] J. Zhang, F. H. B. Lima, M. H. Shao, K. Sasaki, J. X. Wang, J. Hanson, R. R. Adzic, *J. Phys. Chem. B* **2005**, *109*, 22701 – 22704.
[15] J. A. Horsley, *J. Chem. Phys.* **1982**, *76*, 1451 – 1458.
[16] A. N. Mansour, J. W. Cook, D. E. Sayers, *J. Phys. Chem.* **1984**, *88*, 2330 – 2334.
[17] A. N. Mansour, D. E. Sayers, J. W. Cook, D. R. Short, R. D. Shannon, J. R. Katzer, *J. Phys. Chem.* **1984**, *88*, 1778 – 1781.
[18] F. M. F. de Groot, M. H. Krisch, J. Vogel, *Phys. Rev. B* **2002**, *66*, 195112.
[19] O. V. Safonova, M. Tromp, J. A. van Bokhoven, F. M. F. de Groot, J. Evans, P. Glatzel, *J. Phys. Chem. B* **2006**, *110*, 16162 – 16164.
[20] J. K. Nørskov, J. Rossmeisl, A. Logadottir, L. Lindqvist, J. R. Kitchin, T. Bligaard, H. Jonsson, *J. Phys. Chem. B* **2004**, *108*, 17886 – 17892.
[21] S. R. Brankovic, J. X. Wang, R. R. Adzic, *Surf. Sci.* **2001**, *474*, L173 – L179.
[22] H. F. Waibel, M. Kleinert, L. A. Kibler, D. M. Kolb, *Electrochim. Acta* **2002**, *47*, 1461 – 1467.
[23] S. Strbac, S. Petrovic, R. Vasilic, J. Kovac, A. Zalar, Z. Rakocevic, *Electrochim. Acta* **2007**, *53*, 998 – 1005.
[24] M. Duisberg, M. Dräger, K. Wandelt, E. L. D. Gruber, M. Schmid, P. Varga, *Surf. Sci.* **1999**, *433*, 554 – 558.
[25] D. Friebel, D. J. Miller, C. P. O'Grady, T. Anniyev, J. Bargar, U. Bergmann, H. Ogasawara, K. T. Wikfeldt, L. G. M. Pettersson, A. Nilsson, *Phys. Chem. Chem. Phys.* **2011**, *13*, 262 – 266.
[26] E. Bauer, J. H. van der Merwe, *Phys. Rev. B* **1986**, *33*, 3657 – 3671.
[27] A. L. Ankudinov, B. Ravel, J. J. Rehr, S. D. Conradson, *Phys. Rev. B* **1998**, *58*, 7565 – 7576.
[28] H. You, D. J. Zurawski, Z. Nagy, R. M. Yonco, *J. Chem. Phys.* **1994**, *100*, 4699 – 4702.
[29] G. Jerkiewicz, G. Vatankhah, J. Lessard, M. P. Soriaga, Y. S. Park, *Electrochim. Acta* **2004**, *49*, 1451 – 1459.
[30] J. Greeley, J. Nørskov, *Electrochim. Acta* **2007**, *52*, 5829 – 5836.
[31] B. L. Abrams, P. C. K. Vesborg, J. L. Bonde, T. F. Jaramillo, I. Chorkendorff, *J. Electrochem. Soc.* **2009**, *156*, B273 – B282.
[32] Y. Gohda, A. Gross, *J. Electroanal. Chem.* **2007**, *607*, 47 – 53.
[33] M. Ø. Pedersen, S. Helveg, A. Ruban, I. Stensgaard, E. Lægsgaard, J. K. Nørskov, F. Besenbacher, *Surf. Sci.* **1999**, *426*, 395 – 409.
[34] M. Todorova, W. X. Li, M. V. Ganduglia-Pirovano, C. Stampfl, K. Reuter, M. Scheffler, *Phys. Rev. Lett.* **2002**, *89*, 096103.

